

Provided for non-commercial research and education use.
Not for reproduction, distribution or commercial use.



This article appeared in a journal published by Elsevier. The attached copy is furnished to the author for internal non-commercial research and education use, including for instruction at the authors institution and sharing with colleagues.

Other uses, including reproduction and distribution, or selling or licensing copies, or posting to personal, institutional or third party websites are prohibited.

In most cases authors are permitted to post their version of the article (e.g. in Word or Tex form) to their personal website or institutional repository. Authors requiring further information regarding Elsevier's archiving and manuscript policies are encouraged to visit:

<http://www.elsevier.com/copyright>



The role of simvastatin in the osteogenesis of injectable tissue-engineered bone based on human adipose-derived stromal cells and platelet-rich plasma

Yongsheng Zhou^{a,b,*}, Yongwei Ni^a, Yunsong Liu^a, Baijin Zeng^a, Yongwei Xu^a, Wenshu Ge^a

^a Department of Prosthodontics, Peking University School and Hospital of Stomatology, Beijing 100081, PR China

^b Core Laboratory, Peking University School and Hospital of Stomatology, Beijing 100081, PR China

ARTICLE INFO

Article history:

Received 4 February 2010

Accepted 15 March 2010

Available online 9 April 2010

Keywords:

Simvastatin

Adipose-derived stromal cells

Platelet-rich plasma

Bone tissue engineering

Critical-sized calvarial defects

Injectable bone

ABSTRACT

An injectable tissue-engineered bone (ITB) composed of human adipose-derived stromal cells (hADSCs) and platelet-rich plasma (hPRP) was preliminarily constructed, but its osteogenic capability needs improving. This study aimed to evaluate if simvastatin can be applied as a bone anabolic agent for this ITB. We found 0.01 μM , 0.1 μM , and 1 μM simvastatin could induce hADSCs' osteoblastic differentiation *in vitro* that accompanied with non-inhibition on cell proliferation, high alkaline phosphatase activity, more mineralization deposition and more expression of osteoblast-related genes such as osteocalcin, core binding factor $\alpha 1$, bone morphogenetic protein-2, vascular endothelial growth factor, and basic fibroblast growth factor. Simvastatin at 1 μM seemed the most optimal concentration due to its high osteocalcin secretion in media ($P < 0.01$). Quantitative mineralization assay also showed 1 μM SIM had the most obvious synergistic effect on hPRP's induction for matrix mineralization of hADSCs ($P < 0.01$). When 1 μM Simvastatin was applied to this ITB to restore the critical-sized calvarial defects in mice, more bone formation was observed in defected regions, and the peripheries just outside the defect margins by X-ray analysis, and H&E staining. These findings indicate that simvastatin at optimal concentrations can be used to promote this ITB's osteogenesis. However, simvastatin's effects on this ITB await long-term investigation.

© 2010 Elsevier Ltd. All rights reserved.

1. Introduction

An injectable tissue-engineered bone (ITB) composed of human adipose-derived stromal cells (hADSCs) and human platelet-rich plasma (hPRP) was constructed in our previous study [1]. This ITB is more feasible for clinical use because the two ingredients can be easily obtained from autologous resources with large quantity and minimal donor site morbidity [1–5]. Moreover, in the cell proliferation and osteogenic inducing procedures, hPRP is used to eliminate the influence of foreign protein (like fetal bovine serum, etc.), and glucocorticoid (dexamethasone) [1,4]. Furthermore the liquid hPRP and hADSCs can be applied by injection and grafted in minimally invasive way and exhibit excellent plasticity [1,5,6]. Once hPRP is implanted and activated, it will form fibrin scaffold which support the cells growth and differentiation, and released the growth factors slowly [6–8]. Furthermore, the hPRP-formed scaffold also exhibits excellent biodegradability, commensurate with new bone formation [6–9]. This has been successfully confirmed in

preliminary clinical trials of ITB composed of human bone marrow derived mesenchymal stem cells (BMSCs) and hPRP [8,9]. However, hPRP, a multifactorial agent [4–6], is not bone-specific and strong enough when it is used as bone anabolic factor for hADSCs [1]. As we know, recombinant growth factor, such as bone morphogenetic protein (BMP)-2, is a strong osteoinductive agent [10]. However, there are some disadvantages such as complicated synthesis, easy degradation, and expensiveness in its application [10–12]. Moreover, its biological safety is still questioned due to symptomatic ectopic bone formation, bone resorption or remodeling at the graft site, and other potential theoretical complications including tumorigenic and teratogenic effects [11,12]. Although genetically modified mesenchymal stem cells (MSCs) are also promising for enhancing bone formation, their biological safety, cost and availability are also questioned for their complex gene transduction procedures and the incorporation of exogenous genes into the genome [13]. Therefore, a simplified, safe, cost-effective and reliable drug instead of a recombinant growth factor is expected to improve hPRP's bone anabolic effects when this ITB only composed of hADSCs and hPRP is constructed. Therefore, further researches should be applied to confirm this possibility.

Simvastatin (SIM), an inhibitor of the competitive 3-hydroxy-3-methyl coenzyme A (HMG-CoA) reductase, is a convenient and

* Corresponding author. Department of Prosthodontics, Peking University School and Hospital of Stomatology, Beijing 100081, PR China. Tel.: +86 10 62179977x2370; fax: +86 10 62173402.

E-mail address: kqzhouysh@hsc.pku.edu.cn (Y. Zhou).

economical drug which has been widely used to treat hyperlipidemic [14–16]. Since Mundy et al. discovered that statins can stimulate high expression of bone morphogenetic protein (BMP)-2 in osteoblasts, and can effectively stimulate bone formation after undertaking a thorough screening over 30,000 natural or artificial compounds [14], lots of studies have further confirmed that SIM is a potential drug in the treatment of osteoporosis [15], fracture healing [16], and so on. Therefore, we raise a hypothesis: SIM, which have been safely prescribed to patients for more than 2 decades, can be used to induce the osteoblastic differentiation of hADSCs, and enhance the osteogenic inducing effect of hPRP on hADSCs *in vitro* and *in vivo*. If it is true, that means SIM can be used to enhance the bone formation of this ITB composed of hADSCs and hPRP.

In order to verify this hypothesis, this study was designed to probe into the following contents: (1) the effects of SIM on the proliferation and osteogenic differentiation of hADSCs *in vitro*, and the selection of the appropriate concentration for SIM; (2) the effects of the combined application of SIM and hPRP on the osteogenic potential of hADSCs *in vitro*; (3) the effects of the ITB containing SIM on the restoration of critical-sized calvarial defects in mice.

2. Materials and methods

2.1. Materials

All materials were purchased from Sigma Chemical Co. (St. Louis, MO, USA) unless otherwise stated. Dulbecco's modified Eagle's medium (DMEM) and fetal bovine serum (FBS) were purchased from Hyclone (Logan, UT, USA). Trypsin was purchased from GIBCO/BRL (Carlsbad, CA, USA). Bovine Thrombin was purchased from Calbiochem (Bad Soden, Germany). TRIZOL reagents and Superscript II reverse transcriptase were purchased from Invitrogen (Carlsbad, CA, USA). Oligo dT, Taq DNA polymerase, and dNTP were purchased from Promega (Madison, WI, USA). The primers were synthesized by Shanghai Sangon Biological Engineering Technology and Services Company (Shanghai, China).

2.2. Cell isolation and culture

Human adipose tissues were obtained with informed consents from 5 healthy donors who were under liposuction surgery for esthetic reason in the plastic surgery hospital affiliated to Chinese Academy of Medical Science. The study was approved by the Ethics Committee of the Peking University Health Science Center (PKUHSC), Beijing, China. Human adipose tissue-derived stromal cells (hADSCs) were isolated and cultured according to our previously published articles [1,3]. Cells of the third passage were used for the *in vitro* experiments and all *in vitro* experiments were repeated 3 times using hADSCs from the 3 patients respectively. Cells of the fourth passage from other 2 patients were used for the *in vivo* experiments.

2.3. Preparation and activation of human platelet-rich plasma

Five whole blood samples of healthy adult volunteers (age between 23 and 32) were collected under informed consents. This was also approved by the Ethics Committee of PKUHSC. The human platelet-rich plasma (hPRP) was prepared and

activated according to our previously published paper as well [1]. For each sample, the average platelet concentration of the whole blood was $163 \times 10^9/L$, and the platelet concentration of hPRP was $1025 \times 10^9/L$. The average ratio of platelet concentration for hPRP/whole blood was 6.3. In this study, 10% hPRP was used for *in vitro* test and the preliminary induction of hADSCs before implantation into ITB according to Liu Y's report [1].

2.4. Proliferation and osteogenic differentiation of hADSCs stimulated by simvastatin or/and hPRP *in vitro*

The hADSCs were seeded in 96-well plates (Corning Life Sciences, Acton, MA, USA) at relatively low density (2×10^3 cells/well) for proliferation assay, and were seeded in 24-well plates (Corning Life Sciences, Acton, MA, USA) at relatively high density (2×10^4 /well) for analyses of osteoblastic differentiation. The study groups including different concentrations of SIM were set for the following 6 studies (see Table 1) and nine wells were used for each group in each quantitative study. Each study was repeated in triplicate. To prepare the stock SIM solution, the compound was dissolved in 50 ml of phosphate-buffered saline (PBS) with 2% dimethylsulfoxide and 0.1% BSA [14].

2.4.1. Assessment of the effect of simvastatin on cell proliferation

Cell proliferation analysis for each group (see Table 1) was performed using the MTT assay. After culturing for 0, 1, 3, 5, 7, 9 days, the MTT assay was performed according to the cell proliferation kit protocol (Sigma). This assay is based on the ability of mitochondrial dehydrogenases to oxidize thiazolyl blue (MTT), a tetrazolium salt 3-(4,5-dimethyl-2-thiazolyl)-2,5-diphenyl-2H-tetrazolium bromide, to an insoluble blue formazan product. Then, the optical density (OD) of the plates were read on microplate reader (Bio-Rad Model 550, Hercules, CA, USA) using test and reference wavelengths of 540 and 620 nm, respectively. This test was repeated three times. The growth curves of hADSCs cultured in all groups were drawn.

2.4.2. Alkaline phosphatase activity of SIM-induced hADSCs

The level of ALP activity of each group (see Table 1) was determined on day 6, and 14. Cells were rinsed twice with PBS followed by trypsinization and then scraped into ddH₂O. This was followed by three cycles of freezing and thawing. ALP activity was determined at 405 nm using *p*-nitrophenyl phosphate (pNPP) as the substrate. A 50 μ l sample was mixed with 50 μ l pNPP (1 mg/ml) in 1 M diethanolamine buffer containing 0.5 mM MgCl₂, pH 9.8 and incubated at 37 °C for 15 min on a bench shaker. The reaction was stopped by the addition of 25 μ l of 3 M NaOH per 100 μ l of reaction mixture. Enzyme activity was quantified by absorbance measurements at 405 nm. Total protein content was determined with the BCA method in aliquots of the same samples with the PIERCE (Rockford, Ill, USA) protein assay kit, read at 562 nm and calculated according to a series of albumin (BSA) standards. ALP levels were normalized to the total protein content at the end of the experiment. This test was repeated three times.

2.4.3. Mineralization assays for SIM-induced hADSCs

Matrix mineralization in each group (see Table 1) was determined by staining of alizarin red S on day 14. For quantification of matrix calcification, plates were washed three times with PBS (pH 7.4), then stained with 0.5% alizarin red S in H₂O, pH 4.0, for 1 h at room temperature. After staining, cultures were washed three times with H₂O followed by 70% ethanol. To quantify matrix mineralization, alizarin red S-stained cultures were incubated in 100 mM cetylpyridinium chloride for 1 h to solubilize and release calcium-bound alizarin red S into solution. The absorbance of the released alizarin red S was measured at 562 nm. Data are expressed as units of

Table 1
Concentrations of simvastatin and hPRP in different groups for *in vitro* studies.

| Study | Group | Description | Study | Group | Description | Study | Group | Description |
|--------------------------|-------|------------------|--|-------|------------------|---|-------|---------------------------|
| Cell proliferation assay | 1 | Positive | Assays for detection of osteoblastic differentiation for SIM-induced hADSCs: ALP activity checking, mineralization assay, RT-PCR assay, OC secretion in media. | 1 | Positive | Assay for checking synergistic effect of SIM on mineralization deposition of hADSCs induced by hPRP | 1 | Positive |
| | 2 | 0.01 μ M SIM | | 2 | Negative | | 2 | Negative |
| | 3 | 0.1 μ M SIM | | 3 | 1 nM SIM | | 3 | 10%PRP |
| | 4 | 0.5 μ M SIM | | 4 | 0.01 μ M SIM | | 4 | 10%PRP + 0.01 μ M SIM |
| | 5 | 1 μ M SIM | | 5 | 0.1 μ M SIM | | 5 | 10%PRP + 0.1 μ M SIM |
| | 6 | 2 μ M SIM | | 6 | 1 μ M SIM | | 6 | 10%PRP + 1 μ M SIM |
| | 7 | 5 μ M SIM | | | | | | |
| | 8 | 10 μ M SIM | | | | | | |

In cell proliferation assay, positive group contained DMEM + 10% FBS + antibiotics (100 U/mL penicillin and 100 mg/mL streptomycin).

In assays for detection of osteoblastic differentiation including the assay for checking the synergistic effect of SIM on hPRP, positive group was traditional osteogenic media containing: DMEM + 10% FBS + 100 nM dexamethasone (DEX) + 0.2 mM ascorbic acid + 10 mM β -glycerophosphate + antibiotics. Negative group contained DMEM + 10% FBS + antibiotics. In assays for detection of osteoblastic differentiation of SIM-induced hADSCs, all SIM groups contained: DMEM + 10% FBS + certain concentration of SIM + antibiotics. In assay for checking the synergistic effect of SIM on mineralization deposition of hADSCs induced by hPRP, all SIM groups contained: DMEM + 10% PRP + certain concentration of SIM + antibiotics, whereas 10% PRP group contained no SIM. In assay for detection of OC secretion in culture media of SIM-induced hADSCs and in assay for checking the synergistic effect of SIM on mineralization deposition of hADSCs induced by hPRP, 1 nM SIM group was omitted due to its low inducing effects as other studies showed.

alizarin red S released (1 unit = 1 unit of optical density at 562 nm) per milligram of protein in each culture on a parallel well. This test was repeated three times.

2.4.4. RT-PCR assays for SIM-induced hADSCs

Uninduced and induced culture layers on 3 days after osteogenic induction were rinsed with cold PBS and immediately lysed using Trizol Reagent. Total RNA was isolated and treated by RNase-free DNase I, and quantified by UV spectrophotometry. For RT-PCR analysis of mRNA expression, 1.0 µg of total RNA (in 20 µl reaction volume) was reverse-transcribed using reverse transcriptase (Superscript II) and oligo-dT primers in a standard reaction. The resultant cDNA (1 µl) was then used as template for PCR amplification (in 25 µl reaction volume) of glyceraldehyde-3-phosphate dehydrogenase (GAPDH), core binding factor $\alpha 1$ (Cbfa1), bone morphogenetic protein (BMP)-2, vascular endothelial growth factor (VEGF) and basic fibroblast growth factor (FGF-2). The primers used in this investigation were listed in Table 2 and all primer sequences were determined through established GenBank sequences. 10-µl aliquots of each reaction were evaluated by 1.5% agarose gel electrophoresis. Ethidium bromide-stained gels were digitally photographed (Kodak, Rochester, NY, USA). Amplification of GAPDH was used as an internal control and relative levels for other genes' expression were analyzed with Image J 1.38e (National Institutes of Health, Bethesda, Maryland, USA). All gene expression experiments were performed in duplicate and repeated by hADSCs from individual donors.

2.4.5. Detection of osteocalcin secretion of SIM-induced hADSCs in culture medium

For the quantitative determination of OC secretion at protein level for each group (see Table 1), osteocalcin ^{125}I Radioimmunoassay (RIA) Kit (Chinese Institute of Atomic Energy, Beijing, China) was utilized. This assay was based on a competitive reaction among ^{125}I human OC, sample (culture medium) OC, and rabbit anti-human OC antibodies (polyclonal). After incubation at 4 °C for 20 h, separation solution (a complex of donkey anti-rabbit antibodies, rabbit serum, and polyethylene glycol) was then added into each reaction tube. After incubation for 15 min at room temperature and centrifugation for 15 min at 4 °C, cpm of the deposits was determined by counting machine. OC contents were then calculated according to the standard curve.

2.4.6. Examination of the synergistic effect of SIM on mineralization deposition of hADSCs induced by hPRP

After 14, and 28 days culturing with corresponding media for each group (see Table 1), matrix mineralization of cell layers was determined by staining of alizarin red S on days 14 and 28. The quantitative measurement of matrix calcification for each group was the same as mineralization assays used for SIM-induced hADSCs (see 2.4.3). This was repeated for three times.

2.5. Construction of ITB containing hADSCs, SIM and hPRP

hADSCs were induced with osteogenic medium containing SIM and hPRP (10% hPRP + 1 µM simvastatin + 50 µM ascorbate + 10 mM β -glycerophosphate + DMEM) for 1 week before implantation into the critical-sized calvarial defects of mice. Induced hADSCs (5×10^5 cells) and 0.3 ml hPRP were aspirated into a 1 ml syringe. Here the cells were resuspended directly into hPRP. In a second 1 ml syringe, 1 µM (final concentration after mixing with hPRP) SIM and 100 µL thrombin activators (100 U thrombin was dissolved in 10% CaCl_2 solution) were aspirated. The two syringes were connected with a "T" connector and the plungers of the syringes were pushed and pulled alternatively, allowing the air bubble to expel from the two syringes. The third channel of the "T" connector was connected with a puncture needle. When applying, the two plungers were gently pushed together, allowing the two components to mix adequately and form ITB containing hADSCs, hPRP, and SIM. If SIM was not included in the second syringe, it was used as the positive control group that would form ITB containing hADSCs, and hPRP. If the cells were not included too, the group would be used as another control group that only contained hPRP.

Table 2

Primer sequences of osteoblast-associated genes.

| Gene | Sequence (5'–3') | Size (bp) | Cycle | Annealing temp (°C) |
|----------------|------------------|---------------------------|-------|---------------------|
| GAPDH | Upstream | CAATGACCCCTTCATTGACC | 30 | 60 |
| XM_001725661.1 | Downstream | TGGACTCCACGACGTACTCA | | |
| Osteocalcin | Upstream | GTGCAGAGTCCAGCAAAGGT | 30 | 60 |
| NM_199173.3 | Downstream | TCAGCCAACTCGTCACAGTC | | |
| Cbfa1 | Upstream | GTGGACGAGGCAAGAGTTTCA | 30 | 60 |
| NM_004348.3 | Downstream | CATCAAGCTTCTGTCTGTGCC | | |
| BMP-2 | Upstream | GTCCTGAGCGAGTTCGAGTT | 30 | 58 |
| NM_001200.2 | Downstream | TGAAGCTCTGCTGAGGTGAT | | |
| VEGF | Upstream | CGAAGTGGTGAAGTTCATGGATG | 30 | 60 |
| NM_001033756.1 | Downstream | TTCTGTATCAGTCTTTCCTGGTGAG | | |
| FGF-2 | Upstream | TACAACTTCAAGCAGAAGAG | 30 | 60 |
| NM002006.4 | Downstream | CAGCTCTTAGCAGACATTGG | | |

2.6. Investigation of the osteogenic potential of ITB in vivo

For *in vivo* evaluation, thirty-two 4-week-old BALB/C homozygous nude mice were used (Peking University Experimental Animal Center). All animal experiments were performed in accordance with the institutional animal guidelines. Animals were randomly divided into 4 groups with 8 for each group. Group 1: blank control (negative), i.e. no implantation; Group 2: pure hPRP group (abbreviated as PRP group), i.e. only hPRP gel was implanted; Group 3: hPRP + hADSCs group (abbreviated as PRP + cells group), i.e. ITB containing hADSCs and hPRP; Group 4: ITB containing hADSCs, 1 µM SIM and hPRP (abbreviated as SIM group). Briefly, mice were anesthetized by intraperitoneal injection of 1% pentobarbital with 50 mg/Kg and the surgical sites were cleaned with disinfectant. A 1.0 cm sagittal incision was made on the scalp, and the calvaria were exposed by blunt dissection. A 4 mm-diameter critical-sized defect was created at the right side of the calvarium by means of a trephine bur (Hager Meisinger GmbH, Neuss, Germany) under low speed drilling and copious saline irrigation. The periosteum of the defect region was removed carefully and avoided damage to the dura mater and brain. Occasional bleeding was stopped and the defect regions were washed and the ITB constructs were respectively implanted into the defects, and the incision was closed with suturing. Specimens of each group were harvested at 4 weeks after implantation and animals in each group were sacrificed by CO_2 asphyxiation. The crania were carefully separated and fixed in 4% paraformaldehyde. Soft X-ray examinations were used to evaluate the gray scale levels of ITB. The samples were then decalcified for 10 days in 10% EDTA (pH 7.4). After decalcification, the specimens were dehydrated and subsequently embedded in paraffin. Sections (5 µm-thick) were stained with hematoxylin and eosin (H&E). Osteogenesis of the defect regions and the peripheries just outside the margin of the defects were evaluated as comparing with the healthy contralateral sides of crania of the same mice.

2.7. Soft X-ray detection and gray scale analysis of cranial samples

After fixation with 4% paraformaldehyde, the cranial samples were radiographed with digital radiographic apparatus (GE Senograph 2000D, USA) under condition of 25 KV, 50 mAs, and 50 cm distance. Gray scales of the defect regions and healthy contralateral sides were then analyzed with medical image analyzing software (Image J 1.38e, NIH, USA) and the scales were set between 0 and 255. Compared with the healthy contralateral side of the same mouse, the gray scales were set as 3 levels: level 0: $\leq 1/3$ gray scale value of the healthy contralateral side, indicated no bone formation; level 1: $1/3$ – $2/3$ gray scale value of the healthy contralateral side, indicated possible bone formation; level 2: $\geq 2/3$ gray scale value of the healthy contralateral side, indicated determined bone formation.

2.8. Statistical analysis

Data were analyzed using SPSS version 10.0 (Chicago, Ill, USA). Statistical analysis of the data was performed by one-way analysis of variance (ANOVA) and post-hoc test for multiple comparisons was carried out using the Fisher LSD test. When variance was not homogeneous, Kruskal–Wallis Test was used, followed by Nemenyi test for multiple comparisons. For all tests, statistical significances were accepted for *P* values lower than 0.05.

3. Results

3.1. The effects of different concentrations of SIM on cell proliferation

The cell adhesion to the culture disk, and cell shapes were normal when 1 nM–10 µM SIM was added into the media. The effects of SIM at different concentrations on hADSCs' proliferation

were shown as growth curves (Fig. 1). MTT assays showed that SIM at 2 μM began to slow down the cell growth and the cell proliferation was obviously inhibited when the concentration of SIM in media were higher than 2 μM . SIM under 1 μM (including 1 μM) had negligible adverse influence on the cell proliferation when compared with positive group.

3.2. ALP activities of hADSCs cultured with different concentrations of SIM

ALP activities of all groups varied with culturing duration (Fig. 2). For negative control, ALP activities increased very slowly with culturing days increased. For positive control, ALP activities increased significantly at day 14 when compared with that at day 6. There was no significant difference of ALP activities for all groups at day 6. ALP activities of 0.01 μM , 0.1 μM , and 1 μM SIM groups and positive group were higher than that of negative control and 1 nM SIM group respectively at day 14 ($P < 0.05$), whereas ALP activity of 1 nM SIM group showed no difference with that of negative control group at day 14.

3.3. Matrix mineralization of SIM-induced hADSCs

The effects of SIM at different concentrations on the mineralization of induced hADSCs at day 14 were shown in Fig. 3. Matrix mineralization of 0.01 μM , 0.1 μM , and 1 μM SIM groups and positive group were respectively higher than that of negative control ($P < 0.05$), and 1 nM SIM group ($P < 0.05$). However, only matrix mineralization of 0.01 μM SIM group was higher than that of positive control group ($P < 0.05$), whereas matrix mineralization of 0.1 μM , and 1 μM SIM groups showed no difference with that of positive control ($P > 0.05$).

3.4. Osteoblast-associated genes expression for SIM-induced hADSCs

To confirm osteogenesis, cells were examined by RT-PCR for the expression of several genes (Fig. 4A), including OC, Cbfa1, BMP-2, VEGF and FGF-2. Expression of Cbfa1, BMP-2, VEGF and FGF-2 were observed in all groups including SIM-induced, DEX-induced, or non-induced hADSCs. For the expression of bone-specific gene OC, it was restricted to osteogenic induction (SIM-induced, and DEX-induced), as no basal expression was seen in non-induced negative control. When semi-quantitative comparison was used to analyze the expression of these genes as GAPDH was used as an internal control (Fig. 4B), it was found that SIM at 0.01 μM , 0.1 μM , and 1 μM could obviously upregulate the expression of OC, Cbfa1, BMP-2, VEGF and FGF-2, but 1 nM SIM could not. For positive control, Cbfa1,

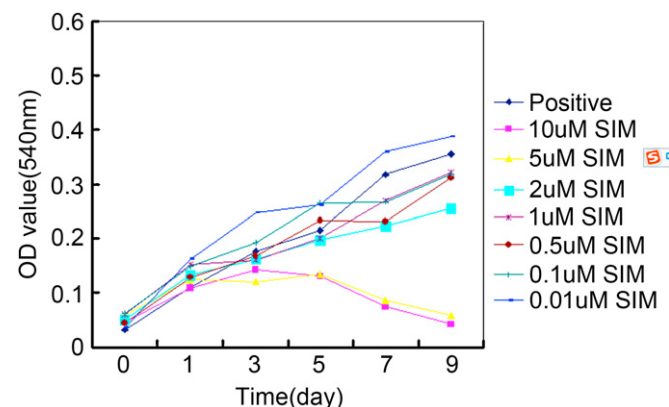


Fig. 1. Growth curves of hADSCs under culturing with different concentrations of SIM.

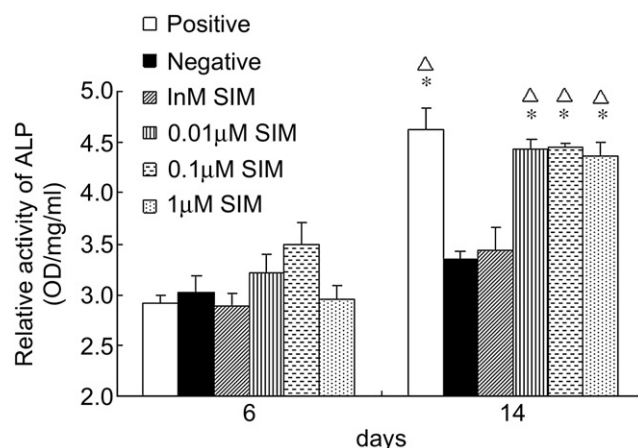


Fig. 2. Relative activities of ALP for hADSCs cultured with different concentrations of SIM at days 6, and 14. *: $P < 0.05$ vs negative group; Δ : $P < 0.05$ vs 1 nM SIM group (Nemenyi test).

and OC were upregulated, but BMP-2, VEGF, and FGF-2 were lowly expressed when compared with negative control.

3.5. Osteocalcin secretion in culture medium by SIM-induced hADSCs

Osteogenesis of SIM-induced hADSCs was also confirmed at the protein level of OC by radioimmunoassay (Fig. 5). At time point of 24, and 72 h, its secretion for 1 μM SIM group was upregulated significantly when respectively compared with negative control ($P < 0.05$), 0.01 μM SIM group ($P < 0.05$), or 0.1 μM SIM group ($P < 0.05$), whereas 0.01 μM group, and 0.1 μM SIM group showed no difference with negative control ($P > 0.05$). However, compared with positive control, its secretion in 1 μM SIM group showed an insignificant increase ($P > 0.05$). When compared with negative control, its secretion in positive control group also showed an insignificant increase ($P > 0.05$).

3.6. SIM's synergistic effects on matrix mineralization of hPRP-induced hADSCs

The synergistic effects of SIM at different concentrations on matrix mineralization of hPRP-induced hADSCs were indicated in Fig. 6. Matrix mineralization for 4 experimental groups (PRP,

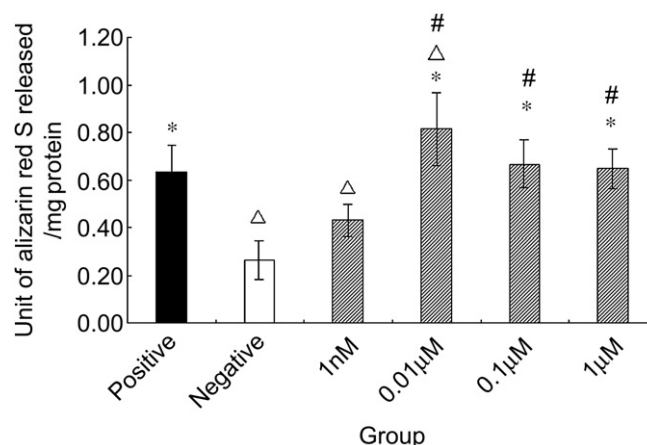


Fig. 3. Quantitative detection of calcification deposition of hADSCs cultured with different concentrations of SIM at day 14. *: $P < 0.05$ vs negative control group. Δ : $P < 0.05$ vs positive control group. #: $P < 0.05$ vs 1 nM SIM group.

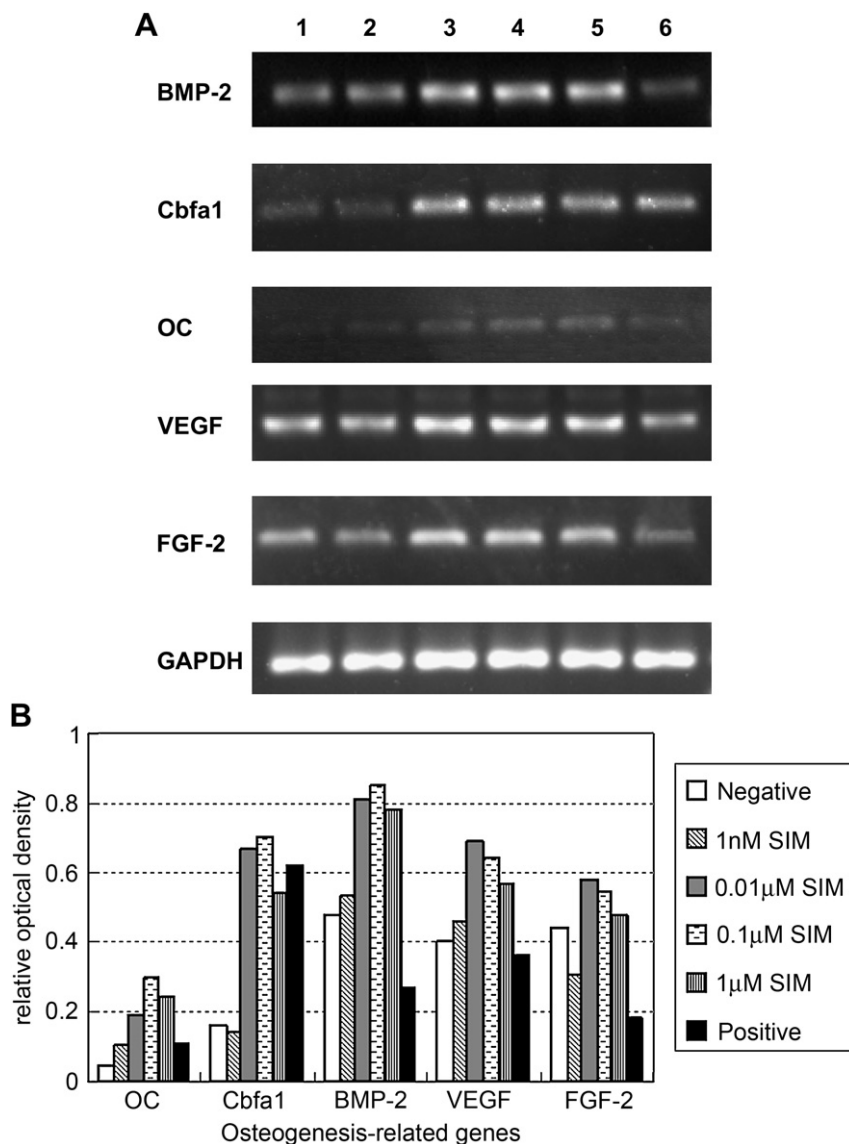


Fig. 4. The effects of different concentrations of simvastatin on the mRNA expression of OC, Cbfa1, BMP-2, VEGF, FGF-2 and GAPDH for hADSCs at 72 h of induction. A: PCR results, 1–6 respectively represented negative, 1 nM SIM, 0.01 µM SIM, 0.1 µM SIM, 1 µM SIM, and positive groups; B: relative mRNA expression of OC, Cbfa1, BMP-2, VEGF, and FGF-2 as expression of GAPDH as an internal control.

PRP + 0.01 µM SIM, PRP + 0.1 µM SIM, and PRP + 1 µM SIM group) and positive control was respectively higher than that of negative control at day 14, and 28 ($P < 0.01$). At day 14, matrix mineralization of these 4 experimental groups were respectively higher than that of positive control ($P < 0.01$), whereas matrix mineralization of 3 experimental groups (PRP, PRP + 0.01 µM SIM, PRP + 0.1 µM SIM) were respectively lower than that of positive control at day 28 ($P < 0.01$) and that of PRP + 1 µM SIM group was not ($P > 0.05$). Matrix mineralization of PRP + 1 µM SIM group was respectively higher than that of other 3 experimental groups at day 14, and 28 ($P < 0.01$).

3.7. Collection and gross observation of calvarial samples

Six mice died during the operation. Other mice suffered no obvious inflammation at surgical sites during the whole stage. Totally, 7 samples from blank control group, 6 samples from PRP group, 6 samples from PRP + cells group, and 7 samples from SIM group were collected in the end. The defected regions of all samples

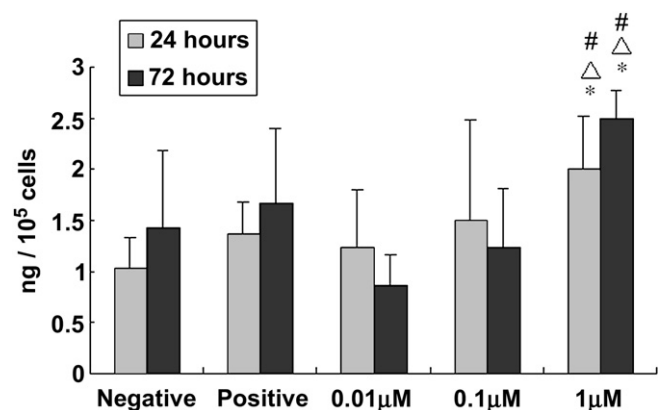


Fig. 5. The osteocalcin secretion of hADSCs cultured in media containing different concentrations of SIM. *: $P < 0.05$ vs negative control at the corresponding time point; Δ: $P < 0.05$ vs 0.01 µM SIM group at the corresponding time point; #: $P < 0.05$ vs 0.1 µM SIM group at the corresponding time point.

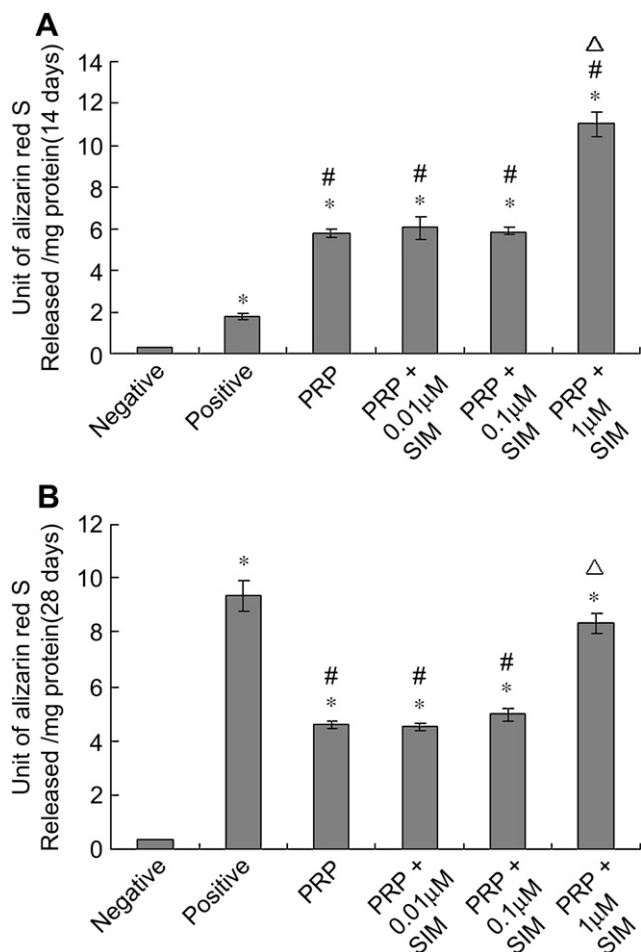


Fig. 6. Quantitative mineralization deposition of hADSCs cultured in media containing 10% PRP and different concentrations of SIM. A: at day 14; B: at day 28. *: $P < 0.01$ vs negative control; #: $P < 0.01$ vs positive control; Δ: $P < 0.01$ vs PRP group, or PRP+0.01 μM SIM group, or PRP+0.1 μM SIM group (Fisher LSD test).

were covered with smooth, continuous soft tissue, and no conglutination was found. Obvious hard tissues (bone formation) were seen in defected regions in SIM group, and PRP + cells group, whereas, only small amount hard tissue was observed in pure PRP group and no hard tissue was observed in blank control group.

3.8. Soft X-ray analysis of calvarial samples

Soft X-ray analyses of calvarial samples were shown in Fig. 7. For blank control group, no high density (bone formation) was observed and the margins of the defects were smooth. For PRP group, very small amount of high density spots were observed and the margins of the defects became not smooth. For PRP + cells group, obvious high density spots or regions were observed and the margin of the defects became not smooth as well. For SIM group, more obvious high density spots or regions were observed and the margins of the defects became more irregular.

3.8.1. Analysis of the relative gray scale percentage of bone defected regions to the healthy contralateral sides based on soft X-ray films

The relative gray scale percentages of the whole critical-sized defected regions (4 mm in diameter, 12,000 pixels circle area) to the corresponding sites of the healthy contralateral sides which reflected osteogenic efficiency were shown in Fig. 8. For SIM group, less than 50% new bone formed after 4 weeks of implantation. The

relative gray scale percentage of SIM group was respectively higher than that of PRP + cells group ($P < 0.05$), pure PRP group ($P < 0.01$), and blank control group respectively ($P < 0.01$). The relative gray scale percentage of PRP + cells group was higher than that of blank control group ($P < 0.01$).

When compared the relative gray scale percentages of the central areas of the defected regions (5000 pixels circle area) of each group, the percentage of SIM group was respectively higher than that of other 3 groups respectively ($P < 0.01$). The percentage of PRP + cells group was higher than that of PRP group, and blank control group respectively ($P < 0.01$).

3.8.2. Gray scale distribution of the critical-sized bone defects

The average gray scale of the healthy contralateral sides of each group was listed in Table 3 and there was no difference of values among these groups ($P > 0.05$). The gray scale distribution of the defect regions for each group was listed in Table 3 as well. The percentage of gray scale at level 1 for PRP + cells group, and SIM group was significantly higher than that of PRP group ($P < 0.01$), and blank control group ($P < 0.01$) respectively, whereas there was no difference between PRP + cells group and SIM group. The percentage of gray scale at level 2 for SIM group was respectively higher than that of other 3 groups ($P < 0.01$); The percentage of gray scale at level 2 for PRP + cells group was significantly higher than that of blank control group ($P < 0.01$), whereas there was no significant difference with that of PRP group ($P > 0.05$).

3.9. Histological analysis of bone formation by H&E staining

Histological changes of the defect regions for each group were shown in Fig. 9. For blank control group, no bone formation was shown in defect regions. For PRP group, only very small amount of osteoid formed. For PRP + cells group, and SIM group, new bone formation with normal bone-like structure was observed. SIM group showed more osteoid formation than PRP group and PRP + cells group, and PRP + cells group showed more osteoid formation than PRP group.

The histological changes in the peripheries just 2 mm outside the defect margins (abbreviated as periphery) were also shown in Fig. 10. For SIM group, lamellar thickness of the peripheries was more than that of other 3 groups respectively and SIM group showed the most obvious new bone formation at its periphery. For PRP + cells group, PRP group, and blank control group, no obvious bone formation was observed at their peripheries.

4. Discussion

4.1. Osteogenic differentiation of hADSCs induced with SIM *in vitro*

There is *in vitro* evidence to show that statins including simvastatin (SIM) can induce osteoblastic differentiation of bone marrow derived mesenchymal precursor cells, and improve the osteogenesis of human or animal osteoblastic cell lines [17–22]. Does SIM have the same effects on the osteoblastic differentiation of hADSCs? Can SIM be applied to accelerate the osteogenesis of ITB composed of hADSCs and hPRP which was preliminarily constructed in our previous animal experiment [1]? In order to answer these questions, *in vitro* investigations should be firstly performed to determine the optimal concentration threshold and the effectiveness of SIM for hADSCs. In this study, MTT test showed SIM under 1 μM (including 1 μM) had no obvious inhibition on the cell proliferation, whereas, SIM above 1 μM began to slow down the cell growth and obviously inhibited the cell growth when its concentration reached 5 μM. Kupcsik L et al. also found statins above 1 μM have a cytotoxic effect on human BMMSCs which was as

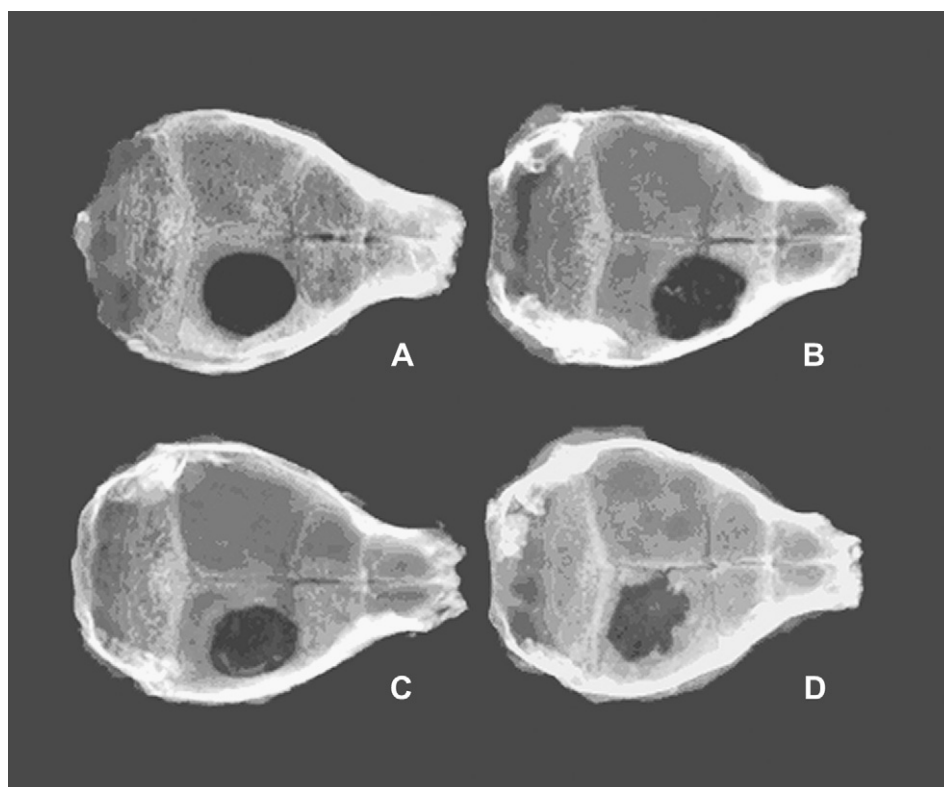


Fig. 7. Bone formation for the critical-sized calvarial defects in mice. A: blank control group; B: PRP group; C: PRP + Cells group; D: SIM group.

a result of cell death [23]. Thus the effect of SIM on cell proliferation of hADSCs was quite similar to that of BMMSCs. Based on cell proliferation test, 1 nM–1 μM SIM was then used to determine if SIM can induce hADSCs to differentiate along osteoblastic lineage and to find the optimal concentration range for its osteogenic induction. The differentiation of hADSCs into osteoblasts was investigated through detection of endogenous ALP enzyme activity, extracellular matrix mineralization, and the expression of osteoblast-associated genes such as OC, Cbfa1, BMP-2, VEGF and FGF-2. When hADSCs were treated with 0.01 μM, 0.1 μM, and 1 μM SIM, elevated ALP enzyme activity, more extracellular mineralization, and the up-regulated expression of OC, Cbfa1, BMP-2, VEGF and FGF-2 were

detected. However, when they were treated with 1 nM SIM, no obvious change of ALP activity, matrix mineralization, and osteoblast-related genes' expression was observed. Because mature osteoblasts are normally characterized by high ALP enzyme activity, matrix mineralization, and osteogenesis-related genes expression [3], we concluded that 0.01 μM, 0.1 μM, and 1 μM SIM can induce osteoblastic differentiation of hADSCs *in vitro*, whereas, 1 nM cannot. Therefore, in our researches of later stage, 1 nM SIM group was omitted. Because OC is a late bone marker that is secreted only by mature osteoblasts and represents terminal osteoblastic differentiation and matrix maturation [24], its expression at protein level was further examined with radioimmunoassay so as to confirm the most optimal concentration. Because only 1 μM SIM could induce significant expression of OC for hADSCs in media, it indicated 1 μM may be the most optimal concentration for the osteogenic induction for hADSCs *in vitro*. In many previous experiments investigating the effects of SIM on osteoblastic differentiation of other cells, similar results were achieved. Baek KH et al. reported that both 0.01 μM SIM and 1 μM SIM could induce the osteogenic differentiation of human BMMSCs, although the two concentrations were found to inhibit the cells' proliferation [17]. For MC3T3-E1 cells, significant osteogenic inducing effects were also observed for SIM at a concentration of 0.1 μM and 0.01 μM, SIM at 0.1 μM showed the maximal effects [18,19]. Ruiz-Gaspa et al. used 1 nM–1 μM SIM to treat a primary human osteoblast and MG-63 cell line and found that SIM had a stimulatory effect on the expression of osteoblast-related genes such as collagen I, OC, and BMP-2 for these cells, although SIM at all the concentrations decreased cell proliferation [20]. Song C et al. used 0–2 μM SIM to stimulate primary cultured bone marrow stromal cells and suggested that SIM can enhance their osteoblastic differentiation and inhibit their adipogenic differentiation [21]. However, Sonobe M et al. used fluvastatin, SIM and pravastatin at only one concentration (0.01 μM)

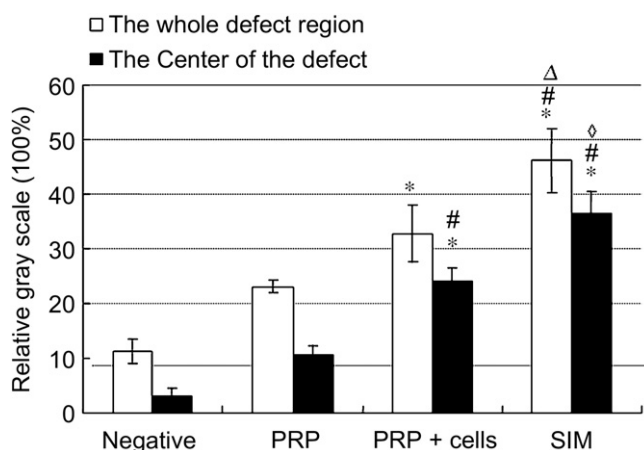


Fig. 8. Relative gray scale of the defects. *: $P < 0.01$ vs blank control (Negative); #: $P < 0.01$ vs PRP group; Δ: $P < 0.05$ vs PRP + cells group; ◇: $P < 0.01$ vs PRP + cells group.

Table 3
Gray scale distribution of the critical-sized calvarial bone defects.

| Groups | Average gray scale value of healthy contralateral side | Gray scale distribution of bone defect regions (percentage) | | |
|---------------------|--|---|----------------|-----------------|
| | | Level 0 | Level 1 | Level 2 |
| Blank (n = 7) | 63.99 ± 5.11 | 92.0 ± 0.83 | 4.50 ± 0.68 | 3.23 ± 0.52 |
| PRP (n = 6) | 61.28 ± 4.88 | 80.74 ± 0.97 | 9.35 ± 1.18 | 9.90 ± 1.34 |
| PRP + cells (n = 6) | 61.79 ± 5.03 | 67.85 ± 5.23 | 18.42 ± 3.45*# | 13.72 ± 2.90* |
| SIM (n = 7) | 60.24 ± 3.99 | 60.35 ± 6.02 | 18.68 ± 2.89*# | 20.97 ± 3.17*#Δ |

Level 0: $\leq 1/3$ gray scale value of the healthy contralateral side, indicated no bone formation.
 Level 1: $1/3-2/3$ gray scale value of the healthy contralateral side, indicated possible bone formation.
 Level 2: $\geq 2/3$ gray scale value of the healthy contralateral side, indicated determined bone formation.
 *: $P < 0.01$ vs blank control; #: $P < 0.01$ vs PRP group; Δ: $P < 0.01$ vs PRP + cells group.

to treat rat BMMSCs and concluded that the statins did not significantly enhance bone formation [22]. Kupcsik L et al. found that SIM lower than $1 \mu\text{M}$ failed to induce calcification of human BMMSCs [23]. It is believed that this discrepancy results from the different culture systems and target cells. Therefore, most *in vitro* studies including our current study indicate that low concentration of SIM can induce osteoblastic differentiation and osteogenesis, although some contradictory results still exist.

It was found that non-induced hADSCs and BMMSCs can express osteogenesis-related genes (mRNA) such as Collagen 1, ALP,

osteopontin, osteonectin, and Cbfa1, and non-induced MSC can also express low level OC which is specific for osteoblastic differentiation [2]. In this study, similar results were achieved. Non-induced hADSCs not only had a relatively low level of endogenous ALP enzyme activity, but also they could express some osteogenesis-related genes such as Cbfa1, VEGF, FGF-2 and BMP-2. This phenomenon may result from their nonspecific characteristics as markers of osteogenesis [2,24]. However, under stimulation of SIM at concentration from $0.01 \mu\text{M}$ to $1 \mu\text{M}$, these genes were found to express with much higher levels when compared with negative

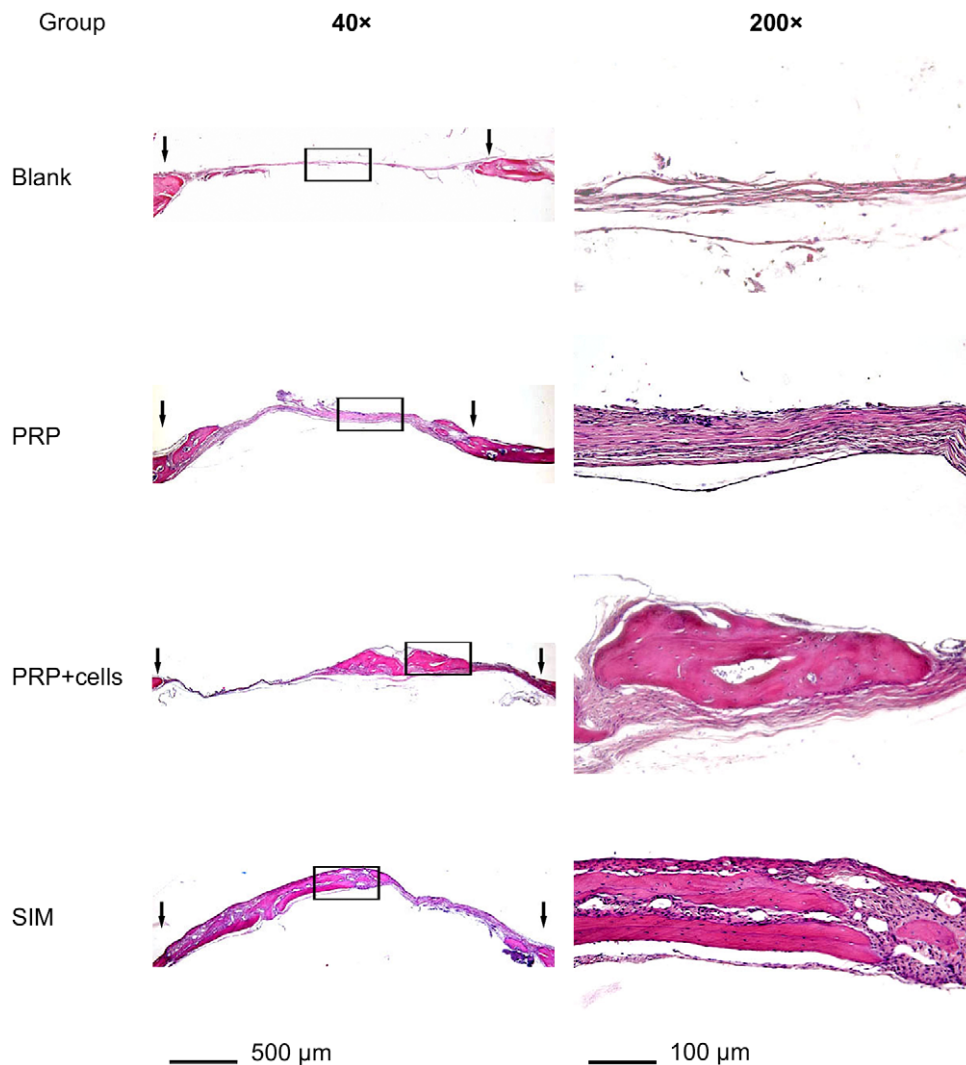


Fig. 9. New bone formation in bone defects at 4 weeks (left: 40× magnification; right: 200× magnification. Black arrow indicated the margin of the bone defects).

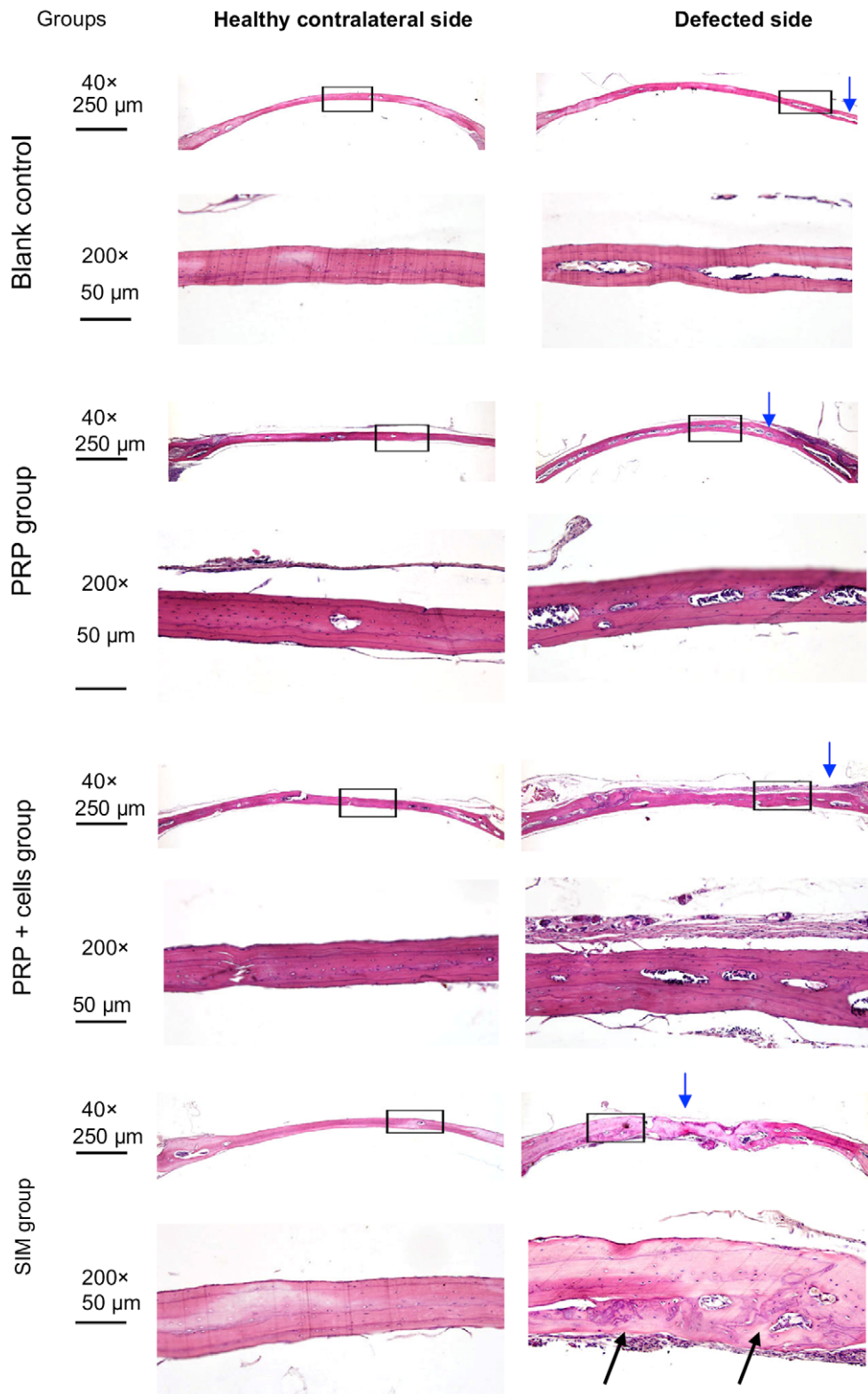


Fig. 10. The thickness of lamellar bone at the peripheries 2 mm outside the defect margins (the right side of blue arrow indicated margin of the bone defects, black arrow indicated new bone formation).

controls, which indicated these genes could be used to signal SIM-induced osteogenesis and even be used to clarify the possible mechanism for this osteogenic process. In this study, osteocalcin, a bone-specific gene, was only shown to express in induced cells

(SIM-induced and DEX-induced) and this indicated its significance in osteoblastic differentiation. For DEX-induced hADSCs, which was used as positive control, they expressed higher level Cbfa1 and OC but lower levels of VEGF, FGF-2 and BMP-2 when compared with

non-induced negative controls. The low level expression of these osteogenesis-related genes may be resulted from the inhibitory effects of dexamethasone which have been confirmed in other researches [2]. However, when the mineralization assay and ALP activity assay were observed, positive control still showed significant higher levels than the negative control. The combined results of these 3 aspects (ALP activity, gene expression, and mineralization) showed that positive control could induce the osteoblastic differentiation of hADSCs as we expected.

The mechanism by which SIM can induce osteogenic differentiation of hADSCs is still unknown. In this study, it was shown that SIM significantly increased BMP-2, Cbfa1, VEGF and FGF-2 mRNA expression. The enhanced expression of BMP-2 mRNA by SIM, which is also a unique characteristic found for other statin-induced cells such as human or rat BMMSCs, MC3T3-E1 [14–21], may be a strong trigger of osteoblast differentiation for hADSCs. Because Cbfa1 is a bone-related transcription factor essential for the differentiation of osteoblast from mesenchymal precursors and bone formation [24], elevated expression of Cbfa1 may also result in the osteoblastic differentiation of hADSCs after stimulation with optimal concentrations of SIM, which was also found for human MSCs stimulated with slow released fluvastatin [25]. It was also demonstrated that statins also have an effect on angiogenesis, a very important process for early stage of new bone formation, by enhancing gene expression for VEGF [19,26,27]. VEGF has also been shown to induce BMP-2 expression, indirectly stimulating osteoblast activity [28]. It was previously reported that basic fibroblast growth factor (FGF-2) stimulates osteoblast differentiation from an early stage through activation of BMP-2 that is mediated by Cbfa1 [29]. It is also a strong angiogenic agent similar to VEGF which can induce angiogenesis a very important early process indispensable for new bone formation [27]. As thus, elevated expression of VEGF and FGF-2 may also result in the osteoblastic differentiation of hADSCs after stimulation with optimal concentrations of SIM. Therefore, SIM may stimulate osteoblast differentiation of hADSCs as a consequence of upregulated expression of BMP-2, Cbfa1, VEGF and FGF-2. However, which factor among these will play the principal role is hard to determine because they may mutually influence each other. BMP-2 can directly induce osteoblastic differentiation by driving the expression of Cbfa1 and vice versa [29]. BMP-2 has also been shown to stimulate the expression of VEGF and vice versa [28,30]. Therefore, the expression of these genes may occur as a result of either a direct action of SIM or via a secondary response due to the increased complementary molecule. So, the effects of SIM on hADSCs may initiate a cascade involving these genes and their ability to activate each other to collectively promote osteogenic differentiation. However, it is noteworthy that this study focused only on the detection of the mRNA expression of these genes, which may not necessarily be an accurate measure of protein levels. Therefore, the osteogenetic mechanism for SIM-induced hADSCs merits further studies.

4.2. The synergistic effect of SIM on osteogenic induction of hPRP for hADSCs *in vitro* and *in vivo*

Based on the *in vitro* optimal concentration range of SIM for osteogenic induction of hADSCs we determined, the synergistic effect of SIM on the osteogenic induction of hPRP for hADSCs was further examined. Because extracellular matrix mineralization is the last phase in the bone developmental sequence and is a specific process in osteoblastic differentiation [24], quantitative matrix mineralization test was performed to check the synergistic effect of SIM on hPRP's osteogenic induction capability *in vitro*. It was confirmed that SIM at 1 μM was still the most optimal concentration to improve hPRP's induction capability. This *in vitro* test did help to

decide the most suitable concentration of SIM which would be used for the subsequent *in vivo* test.

When statins is used as bone anabolic factors *in vivo*, local administration seems more reasonable than systemic administration as currently available statins were targeted toward hepatic metabolism [14,31,32]. They are poorly distributed into bone microenvironment, less than 5% of an oral dose reaches the systemic circulation [32]. Furthermore, low dose of local administration over the defected regions may also help reducing systemic complications of systemically administered statins when taking into account the potential hepatic and renal toxicity associated with these pharmaceuticals [31,32]. Therefore, local application of SIM in this ITB helps keeping the local concentration and provides a safer and more effective pharmacokinetic profile.

In our previous study, ITB only composed of hADSCs and hPRP was constructed and could form bone subcutaneously in mice inguinal grooves. This finding has confirmed its ectopic bone formation capability [1]. In this study, the same ITB, as a positive control, was used to treat the critical-sized calvarial bone defects of mice and was shown to form more bone *in situ* than PRP group and negative group as radiographic and histological examinations showed. When SIM was added into this ITB, new bone formation in defect regions, and the lamellar bone thickness at the peripheral border just outside the defects were significantly increased than that of the positive control group. The reason that the lamellar bone thickness at the peripheral border just outside the defect regions was obviously increased may be due to the diffusing of SIM from the defected region. The *in vivo* synergistic effects of SIM on hPRP's osteogenic induction in this ITB further confirmed the *in vitro* investigations and it was very similar to the local administration of statins on animal calvaria, mandibles and fracture sites [16,31,33]. In these studies, statins were used by direct injection [33], or combination with some carrier systems [16,31], and significant promoting effects on bone formation and healing were achieved. In this study, activated hPRP can form fibrin gel in defect regions which will possibly help to hold SIM and hPRP-released growth factors in site and may possibly maintain this drug and these factors in a slow-release manner [1,6–8]. Conversely, there are some incongruent studies that have shown no significant promoting effects on bone formation and healing for locally administered statins [34,35]. The reasons may possibly result from the applied doses, the applied methods, the local conditions, and pharmacokinetics [31,35]. Pharmacokinetics for lipophilic and hydrophilic statins is different. When hydrophilic statins (such as pravastatin) is directly applied, they may poorly function for osteoprogenitor cells and other bone cells because the active transport system for the uptake of the hydrophilic statins is not present in bone, whereas lipophilicity of lipophilic statins (SIM and lovastatin) facilitate their uptake in bone site [32]. Therefore, for different seed cells and for different applications, optimal concentration and methods for different statins should be firstly considered and investigated. In this study, *in vitro* analyses provided concrete basis for the *in vivo* investigations and we found 1 μM SIM could enhance the bone formation of ITB composed of hADSCs and hPRP *in vivo*. However, new bone formation in bone defects restored with SIM contained ITB, as we noted, was still less than 50% of the healthy contralateral side of calvaria after 1 month implantation. Therefore, the major limitation of this study is that the duration of *in vivo* test should be extended to confirm its long-term osteogenesis. On the other hand, this ITB has low mechanical strength due to the low mechanical characteristic of the fibrin scaffold formed from activated hPRP and it only suits for relatively small defects with bony wall support such as periodontal bone defect which is a very common oral disease. Furthermore, it especially suits for irregular defects because of its injection

feature. Finally, as this ITB is easy to develop and handle, it will have its great potential and prospect.

5. Conclusions

The *in vitro* experiments suggested that simvastatin in optimal concentration can induce human adipose tissue-derived stromal cells to differentiate along the osteoblastic differentiation. Our preliminary *in vivo* data in the mouse models suggest 1 μM simvastatin can be applied to improve the osteogenesis of the injectable tissue-engineered bone composed of human adipose tissue-derived stromal cells and human platelet-rich plasma. However, its long-term osteogenesis should be further investigated in future.

Acknowledgements

We thank Professor Gui-e Ma (Plastic Surgery Hospital affiliated to Chinese Academy of Medical Science, Beijing 100041, PR China) for her kind help in collecting adipose tissues. And we also thank Dr. Shenglin Li (Core Laboratory, Peking University School of Stomatology, Beijing, China) for her technical supports. This study was in part supported by National Natural Science Foundation of China (No. 30200319, No. 30901693), a seed grant of PKU school of stomatology for young scientists.

References

- [1] Liu Y, Zhou Y, Feng H, Ma G, Ni Y. Injectable tissue-engineered bone composed of human adipose-derived stromal cells and platelet-rich plasma. *Biomaterials* 2008;29:3338–45.
- [2] Zuk PA, Zhu M, Ashjian P, De Ugarte DA, Huang JL, Mizuno H, et al. Human adipose tissue is a source of multipotent stem cells. *Mol Biol Cell* 2002;13:4279–95.
- [3] Zhou YS, Liu YS, Tan JG, Is I. 25-dihydroxyvitamin D₃ an ideal substitute for dexamethasone for inducing osteogenic differentiation of human adipose tissue-derived stromal cells *in vitro*? *Chin Med J (Engl)* 2006;119:1278–86.
- [4] Kocaoemer A, Kern S, Klüter H, Bieback K. Human AB serum and thrombin-activated platelet-rich plasma are suitable alternatives to fetal calf serum for the expansion of mesenchymal stem cells from adipose tissue. *Stem Cells* 2007;25:1270–8.
- [5] Ito K, Yamada Y, Nagasaka T, Baba S, Ueda M. Osteogenic potential of injectable tissue engineered bone: a comparison among autogenous bone, bone substitute (Bio-Oss), platelet-rich plasma, and tissue-engineered bone with respect to their mechanical properties and histological findings. *J Biomed Mater Res* 2005;73A:63–72.
- [6] Anitua E, Sánchez M, Nurden AT, Orive G, Andía I. New insights into and novel applications for platelet-rich fibrin therapies. *Trends Biotechnol* 2006;24:227–34.
- [7] Yamada Y, Ueda M, Naiki T, Takahashi M, Hata K, Nagasaka T. Autogenous injectable bone for regeneration with mesenchymal stem cells and platelet-rich plasma: tissue-engineered bone regeneration. *Tissue Eng* 2004;10:955–64.
- [8] Yamada Y, Ueda M, Hibi H, Nagasaka T. Translational research for injectable tissue engineered bone regeneration using mesenchymal stem cells and platelet-rich plasma: from basic research to clinical case study. *Cell Transplant* 2004;13:343–55.
- [9] Kitoh H, Kitakoji T, Tsuchiya H, Mitsuyama H, Nakamura H, Katoh M, et al. Transplantation of marrow-derived mesenchymal stem cells and platelet-rich plasma during distraction osteogenesis: a preliminary result of three cases. *Bone* 2004;35:892–8.
- [10] Wang CK, Ho ML, Wang GJ, Chang JK, Chen CH, Fu YC, et al. Controlled-release of rhBMP-2 carriers in the regeneration of osteonecrotic bone. *Biomaterials* 2009;30:4178–86.
- [11] Benglis D, Wang MY, Levi AD. A comprehensive review of the safety profile of bone morphogenetic protein in spine surgery. *Neurosurgery* 2008;62:ONS423–431.
- [12] Chen NF, Smith ZA, Stiner E, Armin S, Sheikh H, Khoo LT. Symptomatic ectopic bone formation after off-label use of recombinant human bone morphogenetic protein-2 in transforaminal lumbar interbody fusion. *J Neurosurg Spine* 2010;12:40–6.
- [13] Peterson B, Zhang J, Iglesias R, Kabo M, Hedrick M, Benhaim P, et al. Healing of critically sized femoral defects, using genetically modified mesenchymal stem cells from human adipose tissue. *Tissue Eng* 2005;11:120–9.
- [14] Mundy G, Garrett R, Harris S, Chan J, Chen D, Rossini G, et al. Stimulation of bone formation *in vitro* and in rodents by statins. *Science* 1999;286:1946–9.
- [15] Uzzan B, Cohen R, Nicolas P, Cucherat M, Perret GY. Effects of statins on bone mineral density: a meta-analysis of clinical studies. *Bone* 2007;40:1581–7.
- [16] Pauly S, Luttosch F, Morawski M, Haas NP, Schmidmaier G, Wildemann B. Simvastatin locally applied from a biodegradable coating of osteosynthetic implants improves fracture healing comparable to BMP-2 application. *Bone* 2009;45:505–11.
- [17] Baek KH, Lee WY, Oh KW, Tae HJ, Lee JM, Lee EJ, et al. The effect of simvastatin on the proliferation and differentiation of human bone marrow stromal cells. *J Korean Med Sci* 2005;20:438–44.
- [18] Maeda T, Matsunuma A, Kawane T, Horiuchi N. Simvastatin promotes osteoblast differentiation and mineralization in MC3T3-E1 cells. *Biochem Biophys Res Commun* 2001;280:874–7.
- [19] Maeda T, Matsunuma A, Kurahashi I, Yanagawa T, Yoshida H, Horiuchi N. Induction of osteoblast differentiation indices by statins in MC3T3-E1 cells. *J Cell Biochem* 2004;92:458–71.
- [20] Ruiz-Gasca S, Nogues X, Enjuanes A, Monllau JC, Blanch J, Carreras R, et al. Simvastatin and atorvastatin enhance gene expression of collagen type 1 and osteocalcin in primary human osteoblasts and MG-63 cultures. *J Cell Biochem* 2007;101:1430–8.
- [21] Song C, Guo Z, Ma Q, Chen Z, Liu Z, Jia H, et al. Simvastatin induces osteoblastic differentiation and inhibits adipocytic differentiation in mouse bone marrow stromal cells. *Biochem Biophys Res Commun* 2003;308:458–62.
- [22] Sonobe M, Hattori K, Tomita N, Yoshikawa T, Aoki H, Takakura Y, et al. Stimulatory effects of statins on bone marrow-derived mesenchymal stem cells. Study of a new therapeutic agent for fracture. *Biomed Mater Eng* 2005;15:261–7.
- [23] Kupcsik L, Meury T, Flury M, Stoddart M, Alini M. Statin-induced calcification in human mesenchymal stem cells is cell-death related. *J Cell Mol Med*. Postprint 10.1111/j.1582-4934.2008.00545.x.
- [24] Aubin JE, Triffitt JT. Mesenchymal stem cells and osteoblast differentiation. In: Bilezikian JP, Raisz LG, Rodan GA, editors. *The principles of bone biology*. 2nd ed. San Diego: Academic Press; 2002. p. 59–82.
- [25] Benoit DS, Nuttelman CR, Collins SD, Anseth KS. Synthesis and characterization of a fluvastatin-releasing hydrogel delivery system to modulate hMSC differentiation and function for bone regeneration. *Biomaterials* 2006;27:6102–10.
- [26] Weiss M, Heeschen C, Glassford AJ, Cooke JP. Statins have biphasic effects on angiogenesis. *Circulation* 2002;105:739–45.
- [27] Wong RW, Rabie AB. Early healing pattern of statin-induced osteogenesis. *Br J Oral Maxillofac Surg* 2005;43:46–50.
- [28] Bouletreau PJ, Warren SM, Spector JA, Peled ZM, Gerrets RP, Greenwald JA, et al. Hypoxia and VEGF up-regulate BMP-2 mRNA and protein expression in microvascular endothelial cells: implications for fracture healing. *Plast Reconstr Surg* 2002;109:2384–97.
- [29] Choi KY, Kim HJ, Lee MH, Kwon TG, Nah HD, Furuichi T, et al. Runx2 regulates FGF2-induced BMP-2 expression during cranial bone development. *Dev Dyn* 2005;233:115–21.
- [30] Deckers MM, van Bezooijen RL, van der Horst G, Hoogendam J, van Der Bent C, Papapoulos SE, et al. Bone morphogenetic proteins stimulate angiogenesis through osteoblast-derived vascular endothelial growth factor A. *Endocrinology* 2002;143:1545–53.
- [31] Lee Y, Schmid MJ, Marx DB, Beatty MW, Cullen DM, Collins ME, et al. The effect of local simvastatin delivery strategies on mandibular bone formation *in vivo*. *Biomaterials* 2008;29:1940–9.
- [32] Jadhav SB, Jain GK. Statins and osteoporosis: new role for old drugs. *J Pharm Pharmacol* 2006;58:3–18.
- [33] Serin-Kilicoglu S, Erdemli E. New addition to the statin's effect. *J Trauma* 2007;63:187–91.
- [34] Kiliç E, Ozeç I, Yeler H, Korkmaz A, Ayas B, Gümüş C. Effects of simvastatin on mandibular distraction osteogenesis. *J Oral Maxillofac Surg* 2008;66:2233–8.
- [35] Morris MS, Lee Y, Lavin MT, Giannini PJ, Schmid MJ, Marx DB, et al. Injectable simvastatin in periodontal defects and alveolar ridges: pilot studies. *J Periodontol* 2008;79:1465–73.